Experimental and theoretical analyses of RSOA-based colorless-ONUs with 4PAM signal in the up-link

Yueying Zhan (展月英)*, Min Zhang (张 民), Lei Liu (刘 磊), Mingtao Liu (刘明涛), Zhuo Liu (刘 卓), and Xue Chen (陈 雪)

State Key Laboratory of Information Photonics and Optical Communications, Beijing University of Posts and Telecommunications, Beijing 100876, China,

**Corresponding author: zhanyueying@gmail.com*

Received March 5, 2012; accepted May 17, 2012; posted online August 16, 2012

A scheme that utilizes the 4-level pulse-amplitude-modulated (4PAM) signal as the re-modulated signal of colorless optical network units (ONUs) based on reflection semiconductor optical amplifiers (RSOAs) is proposed. The system with 10-Gb/s non-return-to-zero (NRZ) downstream and 5-Gb/s 4PAM upstream signals is theoretically analyzed and experimentally verified. Simulation and experimental results reveal that the 4PAM re-modulated signal yields better performance than the NRZ signal in the upstream. A receiver power penalty of 1.6 dB is also improved by the 4PAM signal at back-to-back (BtB) transmission, whereas another receiver power penalty of 1.5 dB improved after 30-km single mode fiber transmission, where 4PAM signals are used as upstream signal.

OCIS codes: 060.2330, 230.4480, 060.1155.

doi: 10.3788/COL201210.090602.

The demand for high-bandwidth services has fueled the deployment of fiber access networks around the world. Likewise, wavelength-division-multiplexing passive optical network (WDM-PON) with colorless optical network units (ONUs) has attracted considerable attention[1−7]. Recently, various re-modulation schemes for colorless-ONUs based on reflection semiconductor optical amplifiers (RSOAs) have been reported[8−20]. However, these approaches[9−13] have several disadvantages, such as limited RSOA bandwidth and the severe impact of fiber dispersion. Multilevel modulation with higher spectral efficiency is one way of extending the reach of multimode fiber at a high bit rate, although complexity is critical in data communication links. Meanwhile, the 4-level pulse-amplitude-modulated (4PAM) signal offers the lowest implementation complexity in the multilevel modulation format with spectral efficiency of 2 bit/s/Hz[14]. The multilevel signal has been used in the re-modulated signal, which has higher dispersion tolerance than the non-return-to-zero (NRZ) signal; however, the light of the injected signal in RSOA is continuous wave (CW) light[15].

In this letter, we propose a novel wavelength re-modulation scheme for the WDM-PON systems using 10-Gb/s NRZ and 5-Gb/s 4PAM signals in the downstream and upstream, respectively. The feasibility of the proposal is evaluated by experiments and simulations. Simulation and experimental results show that the proposed system with the 4PAM signal has better performance, because it supports higher bit rate and longer distance transmission.

The optical spectra of multilevel signals are typically compressed against the NRZ signal; thus, they have a lower dispersion tolerance than multilevel signals. Figure 1 shows the comparison of the optical spectra between the 4PAM and NRZ signals at 5 Gb/s, wherein the optical spectra of the former comprise half of the optical spectra of the latter. The modulated bandwidth of RSOA is an important limiting factor in the high-rate transmission system.

The rate equations for carriers (N) and total photon density (S) of the RSOA are respectively given by[21,22]

$$\frac{\mathrm{d}N}{\mathrm{d}t} = \frac{J}{eV} - [(A_{\mathrm{rad}} + A_{\mathrm{nrad}})N + (B_{\mathrm{rad}} + B_{\mathrm{nrad}})N^2 + C_{\mathrm{aug}}N^3] - \quad \nu_{\mathrm{g}} g(N,S)S, \tag{1}$$

$$\frac{\mathrm{d}S}{\mathrm{d}t} = \frac{P_{\mathrm{in}}\eta}{h\nu V} + \beta \quad (B_{\mathrm{rad}} + B_{\mathrm{nrad}})N^2 + \mu \quad \nu_{\mathrm{g}} g(N,S)S - \alpha_{\mathrm{int}}\nu_{\mathrm{g}} S, \tag{2}$$

where $S = S^{+\mathrm{ASE}} + S^{-\mathrm{ASE}} + S_{\mathrm{i}}^{+} + S_{\mathrm{i}}^{-}$, $S^{\pm\mathrm{ASE}}$, and $S_{\mathrm{i}}^{\pm}$ are the spontaneously amplified emitted photon density and input photon density of the right and left facets of RSOA, respectively; J is the injection current of the RSOA; A_{rad}, A_{nrad}, B_{rad}, B_{nrad}, and C_{aug} are the recombination coefficients of the RSOA, which are constant; is the optical confinement factor; ν_{g} is the group velocity; β is the spontaneous emission factor; α_{int} is the internal waveguide loss; e is the elementary charge of the electron; V is the active region volume. Expressing the carrier density N as the sum of a steady state term $\overline{N}$

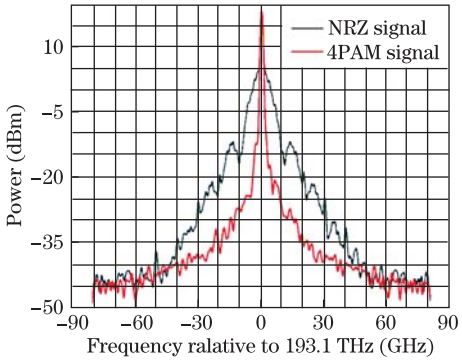

Fig. 1. (Color online) Optical spectra of the NRZ and 4PAM signals.

and a perturbation term $\delta N(t)$ (which follows the formalism $N=\overline{N}+\delta N(t)$, $S=\overline{S}+\delta S(t)$, and $J=\overline{J}+\delta J(t)$) is useful in converting the RSOA nonlinear equations into a linear equation system, facilitating its treatment in the frequency domain. We set the expressions into Eqs. (1) and (2). The new carrier and photon rate equations transferred by the Fourier transfer function are expressed as

$$(\mathrm{j}\omega)\delta N(\omega)=\frac{\delta J(\omega)}{eV}-[(A_{\mathrm{rad}}+A_{\mathrm{nrad}})+2(B_{\mathrm{rad}}+B_{\mathrm{nrad}})\cdot\overline{N}+3C_{\mathrm{aug}}\overline{N}^2+\nu_{\mathrm{g}}g(\overline{N},\overline{S})\overline{S}]\delta N(\omega)-\nu_{\mathrm{g}}g(\overline{N},\overline{S})\delta S(\omega), \tag{3}$$

$$(\mathrm{j}\omega)\delta S(\omega)=[2\beta(B_{\mathrm{rad}}+B_{\mathrm{nrad}})\overline{N}+\mu\nu_{\mathrm{g}}g(\overline{N},\overline{S})\overline{S}]\delta N(\omega)+[\mu\nu_{\mathrm{g}}g(\overline{N},\overline{S})-\alpha_{\mathrm{int}}\nu_{\mathrm{g}}]\delta S(\omega). \tag{4}$$

We then deducted the expression of the small signal response function of the RSOA from Eqs. (3) and (4):

$$G(\omega)=\frac{XZ(UY-VX)}{\sqrt{(\omega^2+VX-UY)^2+\omega^2(Y+U)^2}}. \tag{5}$$

Moreover, the 3-dB bandwidth of the RSOA was defined as the half of peak value of the small signal response. Thus, we obtain the expression of the 3-dB bandwidth as

$$\Delta f_{3\mathrm{dB}}=\frac{1}{2\pi}\sqrt{\frac{\sqrt{12(UY-VX)(Y+U)^2-3(Y+U)^4}-(Y+U)^2+2(UY-VX)}{2}}, \tag{6}$$

$$\Delta f_{3\mathrm{dB}}=\frac{1}{2\pi}\cdot\sqrt{\frac{(\mu m+m\bar{S}+b-c)\sqrt{4m(\mu c+a+b\bar{S})+m^2(6\mu\bar{S}-\mu^2-\bar{S}^2)-(b+c)^2}+m^2[(\bar{S}-\mu)^2+4bc]+2m(a+b\bar{S}+\mu c)-(b+c)^2}{2}}, \tag{7}$$

where $X=2\beta(B_{\mathrm{rad}}+B_{\mathrm{nrad}})\overline{N}+\mu\nu_{\mathrm{g}}g(\overline{N},\overline{S})\overline{S}$, $Z=\frac{1}{eV}$, $Y=\mu\nu_{\mathrm{g}}g(\overline{N},\overline{S})-\alpha_{\mathrm{int}}\nu_{\mathrm{g}}$, $V=-\nu_{\mathrm{g}}g(\overline{N},\overline{S})$, $U=(A_{\mathrm{rad}}+A_{\mathrm{nrad}})+2(B_{\mathrm{rad}}+B_{\mathrm{nrad}})\overline{N}+3C_{\mathrm{aug}}\overline{N}^2+\nu_{\mathrm{g}}g(\overline{N},\overline{S})\overline{S}$, $m=\nu_{\mathrm{g}}g(\overline{N},\overline{S})$, $a=2\beta(B_{\mathrm{rad}}+B_{\mathrm{nrad}})\overline{N}$, $b=\alpha_{\mathrm{int}}\nu_{\mathrm{g}}$, and $c=(A_{\mathrm{rad}}+A_{\mathrm{nrad}})+2(B_{\mathrm{rad}}+B_{\mathrm{nrad}})\overline{N}+3C_{\mathrm{aug}}\overline{N}^2$. The 3-dB bandwidth are related to the state carrier density $\overline{N}$, the state photons density $\overline{S}$, and the injection current $\overline{J}$ of the RSOA. We then set the expressions of X, U, Y, V into Eq. (6) to obtain the relationship between $\overline{S}$ and the 3-dB bandwidth of RSOA given in Eq. (7). The 3-dB bandwidth of RSOA becomes proportional to the photon density using Eq. (7). Assuming that the input binary sequence consists of ideal NRZ pulses with height H and period T, the power spectral density of the 4PAM signal is given by $P(f)=\frac{9H^2T}{4}\sin c^2(3fT)$[23]. Thus, the photon density of the 4PAM signal is higher than that of the NRZ signal at the same input power. Accordingly, the 3-dB bandwidth of the RSOA becomes larger at a higher photon density when the input power and bit rate are the same between the 4PAM and NRZ signals.

Based on the above analysis, we used the 4PAM signal as the re-modulated signal of the RSOA-based colorless-ONU system due to its high photon density and spectra compression. The aim is to increase the operating speed of the WDM-PON system and the limit bandwidth of RSOA. The 3-dB bandwidth of commercial RSOA is approximately 2.2 GHz. The curve of frequency response is shown in Fig. 2, wherein the input optical power is −5 dBm, and the bias current is 65 mA at 1 550 nm.

The encoding method of the 4PAM signal used in our scheme has already been reported[14]. The original data sequence $\{b_k\}$ is pre-coded into the binary sequence $\{d_k\}$, in accordance with

$$d_k=b_k\oplus d_{k-1}\oplus d_{k-2}. \tag{8}$$

The data sequence $\{p_k\}$ of the 4PAM signal is encoded by

$$p_k=d_k+d_{k-1}+d_{k-2}. \tag{9}$$

The proposed WDM-PON architecture is illustrated in Fig. 3. Several distributed feedback (DFB) lasers with different wavelengths were modulated by Mach-Zehnder modulator (MZM) using 10-Gb/s pseudo-random binary sequence (PRBS); these generated the NRZ signal with a downstream signal. The generated downstream signals were then sent to a multiplexer (MUX) and transmitted over a single-mode fiber (SMF). Unlike the downstream signal, which arrived at the ONUs through a demultiplexer (DEMUX), different wavelength lights were sent to different ONUs. A part of the downstream signal at the ONU was fed into the down-link receiver, while another part was injected into the RSOA as upstream signal and was re-modulated as a 5-Gb/s pre-coding NRZ or 4PAM signal. A circulator separated the downstream and upstream signals after fiber transmission at the optical line terminal (OLT). The re-modulated NRZ or 4PAM signal was sent to a DEMUX along SMF and then de-multiplexed. The up-link signals were then

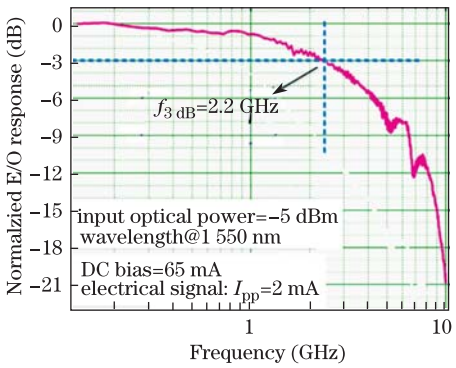

Fig. 2. Frequency response of RSOA.

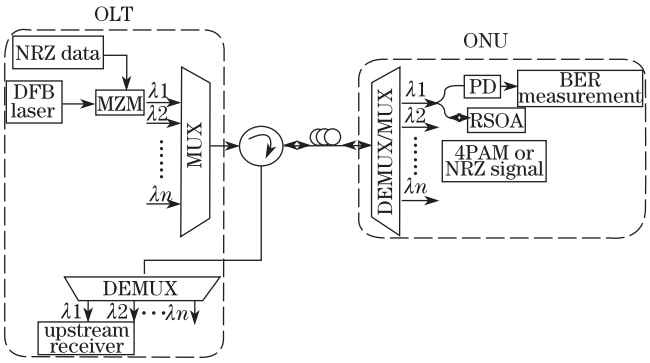

Fig. 3. Architecture of the proposed WDM-PON system. PD: photodiode. BER: bit error rate.

received by the upstream receiver and immediately processed offline.

Figure 4 shows the simulation setup of the proposed WDM-PON system. The NRZ signal for the downstream system was generated by modulating the CW light at λ=1 552.5 nm in a $LiNbO_3$ modulator with 10-Gb/s PRBS. The average power of the CW light was 7 dBm. The NRZ and 4PAM signals for the up-link were generated by re-modulating the down-link signal in RSOA with 5-Gb/s PRBS after pre-coding. The 4PAM optical signal was obtained by applying a 4-level electrical signal to the RSOA. The modulated bandwidth of a 4PAM signal was scaled by 1/2 of the binary signal, which operated at the same bit rate. The average power of the NRZ signal injected into RSOA was −11.4 dBm. The key parameters of the RSOA are listed in Table 1.

Table 1. Parameters of RSOA

Physical Parameters	Value
Device Section Length (m)	500×10^{-6}
Confinement Factor	0.3
Right Facet Reflectivity	0.99
Left Facet Reflectivity	1×10^{-5}
Linear Recombination (s^{-1})	1.0×10^{8}
Initial Carrier Density (m^{-3})	2.0×10^{24}
Group Effective Index	3.7
Gain Coefficient Linear	30×10^{-21}

The BER of these two schemes are shown in Fig. 5, with the following fiber transmission distances back-to-back (BtB), 20 km, and 40 km between NRZ-NRZ and NRZ-4PAM systems. The method of calculated error was programmed with binary patterns that correspond to each level. This pattern was then used to calculate the aggregate symbol error rate (SER) and bit error rate (BER) to measure the SER on each level[14]. The optical spectra of the 4PAM signal was half of the NRZ signal spectra and required a smaller re-modulated bandwidth in the RSOA-based colorless ONU. Thus, the received power penalty of about 1.70 dB was improved at a BER of 10^{-6} after 20-km transmission between NRZ-NRZ system and NRZ-4PAM system. Figure 5 shows the comparison between the BER of the system when the downstream light is un-modulated, and that of a 10-Gb/s NRZ when the downstream light is shown.

Figure 6(a) shows BER at different bit rates ranging from 1 to 8 Gb/s after fiber transmission of 20 km. The performance of the NRZ signal is better than that of the 4PAM signal at bit rates lower than 3 Gb/s. However, the NRZ signal performs poorly compared with the 4PAM signal at bit rates higher than 3 Gb/s. A comparison between BER and the received power of upstream signals at 2.5 and 5 Gb/s is shown in Fig. 6(b). Apparently, the NRZ signal yields better performance at low bit rates, whereas it yields worse performance at high bit rates.

Another way to characterize the quality of digital signals degraded by deterministic distortions is to determine the eye opening penalty (EOP). EOP is defined as the ratio of the eye opening (EO) of the non-distorted reference eye (EO_{ref}) and the EO of the distorted eye[13]. The reference eye diagram in our simulation scheme was obtained when the upstream signal transmission was 20-km SMF fiber. The dispersion coefficient of the fiber was 16×10^{-6} s/m^2, the dispersion was 0.32 s/m, and the EOP was set at 0 dB. We also changed the dispersion coefficient of the fiber. A comparison of the EOP and the dispersion with different 5 Gb/s upstream signals are shown in Fig. 7. As can be seen, the EOP is approximately equal to the received NRZ and 4PAM signals at OLT when the dispersion is less than 0.78 s/m; however, the EOP of the NRZ signal exceeds that of the 4PAM signal when the dispersion is larger than 0.78 s/m.

An analysis of the influence of the signal formats and the extinction ratio (ER) on the performance of the proposed system was also conducted. The performance curve of downstream signal at different ERs is described

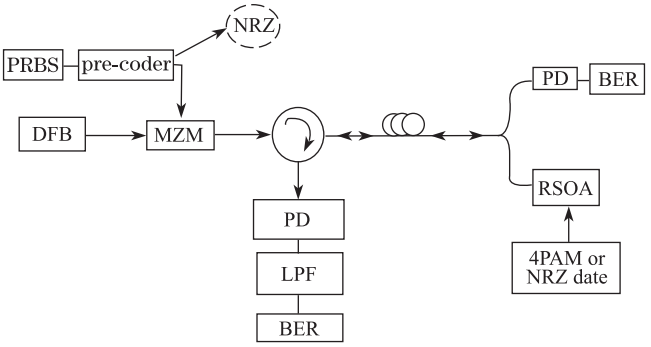

Fig. 4. Simulation setup. LPF: low-pass fiber.

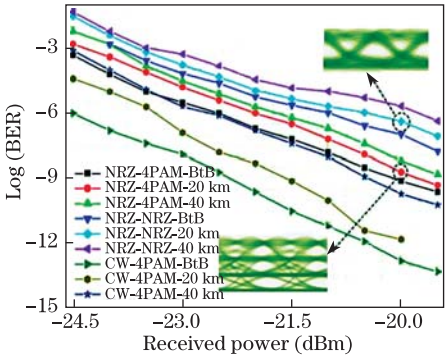

Fig. 5. BER of upstream signals in the NRZ-NRZ system, NRZ-4PAM system, and CW-4PAM system with different fiber distances.

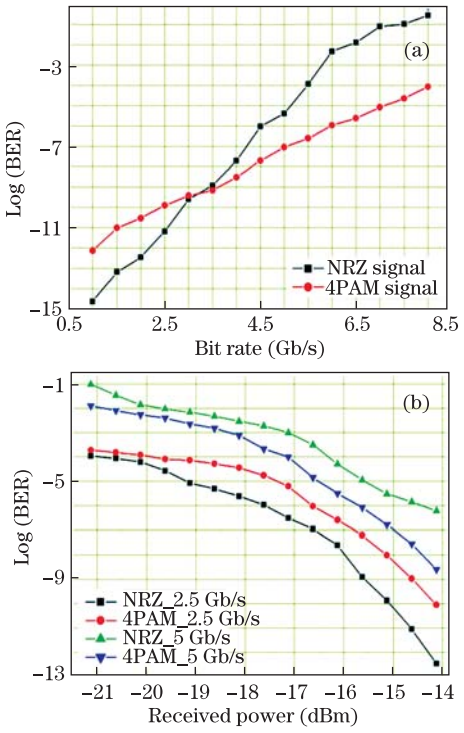

Fig. 6. BER of upstream signals in the NRZ-NRZ system and NRZ-4PAM system with different bit rates. (a) BER versus different bit rates; (b) performances of the NRZ and 4PAM signals at 2.5 and 5 Gb/s, respectively.

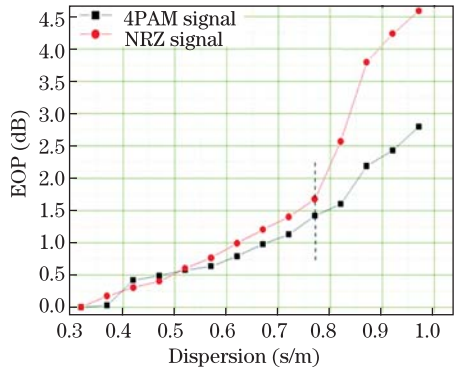

Fig. 7. EOP of the received upstream signals at different dispersions.

in Fig. 8(a). A comparison of the received BER and the ERs of the upstream signals at different bit rates are shown in Fig. 8(b). When the bit rate is lower than 2.5 Gb/s, the performance of the NRZ signal is better than that of the 4PAM signal with increasing ER. However, the 4PAM signal shows better performance when the bit rate reaches 5 Gb/s, because the multilevels require narrower modulation bandwidth than the NRZ signal.

The experiment setup is shown in Fig. 9. In the OLT, a CW light at 1 549.8 nm was introduced into a MZM where a 10-Gb/s NRZ downstream signal was generated by MP1800A of Anritsu. An erbium-doped fiber amplifier (EDFA) compensated for the losses of the MZM at the OLT. The downstream signal was then separated by a coupler after the downstream fiber transmission. One part of the signal was received by the downstream receiver, while the other was injected into RSOA as upstream light. The average power of the NRZ signal injected into the RSOA was set at −8.7 dBm. In the ONU, the 5-Gb/s 4PAM signal was generated by an AWG2021 of Tektronix by considering 7% forward-error-correction (FEC) overhead for the signal. A code rate of 4.67 Gb/s was used, equivalent to the bit rate of the 64B/66B encoding.

Figure 9(a) shows the waveform of the 4PAM signal. Here, the upstream signal was introduced through a bias-T and a resistor capacitor filter circuit, wherein the 3-dB bandwidth of RSOA became 2.2-dB when biased with 75-mA direct current (DC) and modulated with a current of 2 mA. In the upstream receiver, a photo-receiver used at the OLT was also an avalanche photodiode (APD). The low-pass filter (LPF) with a bandwidth of 0.2 nm was placed after the PD. An electronic equalization was then used after the LPF at the OLT, which consisted of a five-stage feed forward equalization (FFE), clock/data recovery, and a two-stage decision feedback (DFE) with adjustable tap coefficients [DFE(5,2)][18]. The received signal was converted from analog-to-digital (AD) signal. Then, the pre-decision receiving signal was pre-checked to adjust the original signal, the de-coder, and BER measurement. Figures 9(b) and (c) show the received 4PAM signal and the processed 4PAM signal at the OLT, respectively.

The BER of the upstream signal measured in the experiments is shown in Fig. 10. In our experiments, 1×10^6 symbols were used for our BER calculation. A received penalty of 1.6 dB was obtained after the NRZ and 4PAM signals were used as upstream signal BtB transmission, with the receiver sensitivities of −12 and −13.6 dBm, respectively. The experiments were conducted

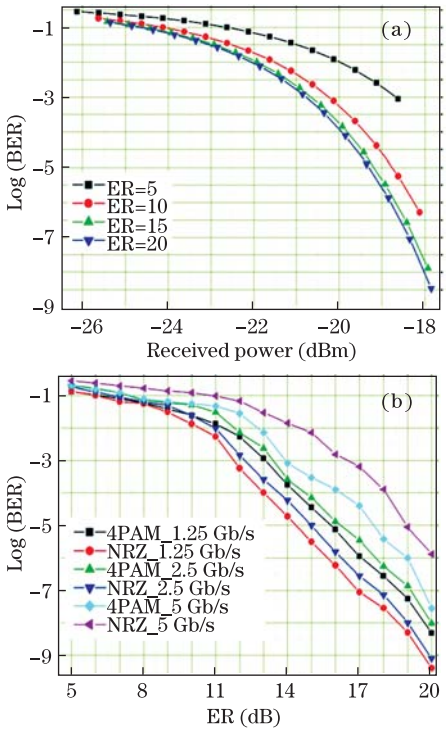

Fig. 8. BER curves at different ERs of the upstream and downstream signals. (a) Performances of downstream signal at different ERs, and (b) received BER versus ER of upstream signal at different bit rates.

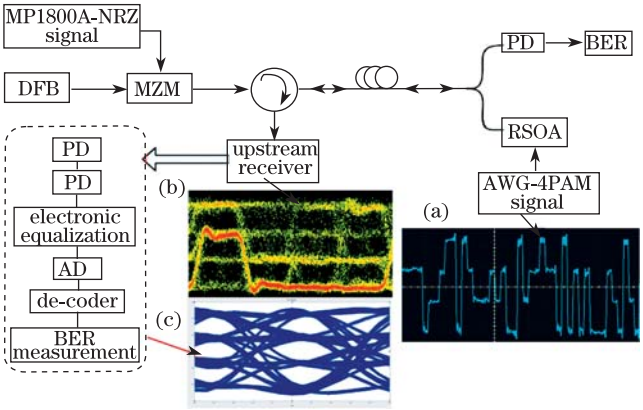

Fig. 9. Experimental setup of the proposed RSOA-based colorless ONU.

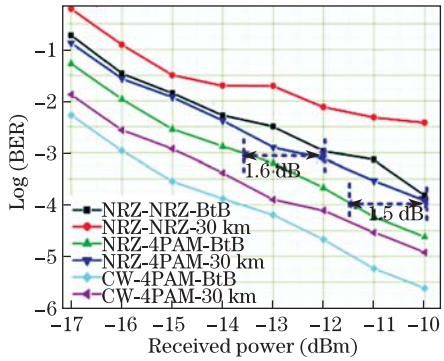

Fig. 10. BER performance of the upstream signal in experiments.

at a BER of 1.0×10^{-3} (i.e., the error-free condition of BER$<10^{-9}$ for Reed-Solomon (255,223) coded). A 2.5-dB power penalty is obtained between the NRZ-4PAM and CW-4PAM systems with BtB experiment. Receiver sensitivity is higher when the upstream is 4PAM signal. However, its receiver sensitivity is degraded as the fiber length increases, and the penalty is at 1.5 dB when we increased the transmission distance to 30 km at BER of 10^{-4}. The experiment result coincides with the above simulation and theoretical analysis.

In conclusion, we propose, simulate, and demonstrate a novel RSOA-based colorless-ONU that utilizes a 10-Gb/s NRZ signal and a 5-Gb/s 4PAM signal in the downstream and upstream, respectively. Simulation and experimental results show that the 4PAM signal has better performance as the re-modulation signal of the RSOA compared with the NRZ signal. Receiver penalty of 1.5 dB is improved after 30-km SMF transmission using the 4PAM signal as the upstream signal. Our scheme is a practical solution for meeting the high data rate and cost-efficient requirements of the optical links in next generation access networks.

This work was supported by the National Natural Science Foundation of China (No. 61072008), the National "863" Program of China (No. 2009AA01Z255), the National "111" Program of China (No. B07005), the New Star Program of Beijing Science and Technology (No. 2007A048), the Fundamental Research Funds for Central Universities (Nos. 2009GYBZ and 2009RC0401), and the Program for Excellent Talents in Beijing University of Posts and Telecommunications.

References

1. J. J. Martínez, J. I. G. Gregorio, A. L. Lucia, A. V. Velasco, J. C. Aguado, and M. Á. L. Binué, J. Lightwave Technol. **26,** 350 (2008).
2. K. Y. Cho, Y. J. Lee, H. Y. Choi, A. Murakami, A. Agata, Y. Takushima, and Y. C. Chung, J. Lightwave Technol. **27,** 1286 (2009).
3. K. Y. Cho, A. Agata, Y. Takushima, and Y. C. Chung, IEEE Photon. Technol. Lett. **22,** 57 (2010).
4. E. Kehayas, B. Schrenk, P. Bakopoulos, J. A. Lazaro, A. Maziotis, J. Prat, and H. Avramopoulos, in *Proceedings of OFC* 2009 OWG4 (2009).
5. C. W. Chow, C. H. Yeh, Y. F. Wu, H. Y. Chen, Y. H. Lin, J. Y. Sung, Y. Liu, and C.-L. Pan, Electron. Lett. **47,** 1235 (2011).
6. L. Liu, M. Zhang, L. Lu, M. Liu, X. Zhang, and P. Ye, Chin. Opt. Lett. **9,** 020606 (2011).
7. M. Omella, V. Polo, J. Lazaro, B. Schrenk, and J. Prat, in *Proceedings of ECOC 2008* Tu.3.E.4 (2008).
8. J. Zhang, X. Yuan, Y. Gu, Y. Huang, M. Zhang, and Y. Zhang, in *Proceedings of ICTON 2009* We.P.1 (2008).
9. T. Duong, N. Genay1, P. Chanclou, B. Charbonnier1, A. Pizzinat1, and R. Brenot, in *Proceedings of ECOC 2008* Th.3.F.1 (2008).
10. H. Kim, IEEE Photon. Technol. Lett. **23,** 965 (2011).
11. G. A. Mahdiraji and E. Zahedi, in *Proceedings of 4th Student Conference on Research and Development* 5 (2006).
12. E. Kehayas, B. Schrenk, P. Bakopoulos, J. A. Lazaro, A.Maziotis1, J. Prat, and H. Avramopoulos, in *Proceedings of OSA / OFC/NFOEC 2010* OWG4 (2010).
13. M. Seimetz, *High-Order Modulation for Optical Fiber Transmission* (Springer, Berlin, 2009).
14. K. Szczerba, P. Westbergh, J. Gustavsson, A. Hanlung, J. Karout, M. Karlsson, P. Andrekson, E. Agrell, and A. Larsson, in *Proceedings of ECOC 2011* Tu.3C.4 (2011).
15. K. Y. Cho, Y. Takushima, and Y. C. Chung, Electron. Lett. **46,** 1510 (2010).
16. H. Kim, in *Proceedings of OFC 2011* OMP8 (2011).
17. H.-C. Kwon, Y.-Y. Won, and S.-K. Han, IEEE Photon. Technol. Lett. **18,** 1852 (2006).
18. M. Omella, I. Papagiannakis, B. Schrenk, D. Klonidis, J. A. Lázaro, A. N. Birbas, J. Kikidis, J. Prat, and I. Tomkos, Opt. Express **17,** 5008 (2009).
19. L. Yi, Z. Li, T. Zhang, D. Lin, Y. Dong, and W. Hu, Chin. Opt. Lett. **9,** 120603 (2011).
20. Y. Qian, M. Zhang, D. Liu, L. Deng, and K. Yang, Chin. Opt. Lett. **8,** 899 (2010).
21. E. Zhou, X. Zhang, and D. Huang, Opt. Express **15,** 9096 (2007).
22. E. S. Björlin, T. Kimura, and J. E. Bowers, IEEE J. Sel. Top. Quantum Electron. **9,** 1374 (2003).
23. S. Walklin and J. Conradi, J. Lightwave Technol. **17,** 2235 (1999).